Journal of Global Change Data & Discovery. 2022, 6(1): 133-141
www.geodoi.ac.cn

20-m/12-d Surface Soil Moisture Dataset for the Panzhuang Irrigation District of China (2020)

Wang, J. J.[1] Zhang, D.[2] Shi, H. J.[3] Lin, R. C.[2] Wang, J.[4] Wei, Z.[2*]

1. Operation and Maintenance Center of Panzhuang Irrigation District, Dezhou 253000, China;
2. China Institute of Water Resources and Hydropower Research, Beijing 100038, China;
3. Water Conservancy Bureau of Dezhou, Dezhou 253014, China;
4. Aerospace Information Research Institute, Chinese Academy of Sciences, Beijing 100101, China

Abstract: Soil moisture is an important factor affecting the energy, water and carbon cycles, agricultural processes, and hydrometeorology. The 20-m/12-d soil moisture dataset covers Panzhuang Irrigation District of China (2020) was developed based on the series of Sentinel-1 SAR images from 2020. A linear regression model was established between the backscattering coefficient and surface soil moisture. Concurrently, the supporting vector machine algorithm based on machine learning was used to identify and extract farmland in the Panzhuang Irrigation District. This dataset includes: (1) boundary vector data for the Panzhuang Irrigation District; and (2) surface soil moisture for 31 12-d periods during 2020, having a temporal resolution of 12 d and a spatial resolution of 20 m. The dataset is archived in .shp and .tif formats and consists of 43 files, amounting to 5.16 GB (or when compressed to 4 files, amounting to 1.09 GB). These data are highly relevant to water storage management, drought warning, and irrigation planning.

Keywords: surface soil moisture; Sentinel-1; back scattering coefficient; the Panzhaung Irrigation District; Shandong

DOI: https://doi.org/10.3974/geodp.2022.01.18

CSTR: https://cstr.escience.org.cn/CSTR:20146.14.2022.01.18

Dataset Availability Statement:

The dataset supporting this paper was published and is accessible through the *Digital Journal of Global Change Data Repository* at: 1https://doi.org/10.3974/geodb.2021.10.08.V1 or https://cstr.escience.org.cn/CSTR:20146.11.2021.10.08.V1.

1 Introduction

Soil moisture (SM) plays an important role in energy, water and carbon cycles, and affects meteorological, hydrological and agricultural processes[1,2]. Surface soil moisture (SSM; 0–5 cm depth) is vital to drought, flood and thunderstorm predictions[3,4]. There are many SSM monitoring methods, e.g., oven-drying[5], modeling[6], and remote sensing estimation[7]. The

Received: 01-11-2021; **Accepted:** 20-12-2021; **Published:** 25-03-2022

Foundations: The special project of China Institute of Water Resources and Hydropower Research (ID0145B052021); Aerospace Information Research Institute, Chinese Academy of Sciences (National Earth Observation Science Data Center Project)

***Corresponding Author:** Wei, Z., China Institute of Water Resources and Hydropower Research, weizheng@iwhr.com

Data Citation: [1] Wang, J. J., Zhang, D., Shi, H. J., *et al*. 20-m/12-d surface soil moisture dataset for the Panzhuang Irrigation District of China (2020) [J]. *Journal of Global Change Data & Discovery*, 2022, 6(1): 133–141. https://doi.org/10.3974/geodp.2022.01.18. https://cstr.escience.org.cn/CSTR:20146.14.2022.01.18.
[2] Wang, J. J., Shi, H. J., Wei, Z., *et al*. 20-m/12-d soil moisture dataset covers Panzhuang Irrigation District of China (2020) [J/DB/OL]. *Digital Journal of Global Change Data Repository*, 2021. https://doi.org/10.3974/geodb.2021.10.08.V1. https://cstr.escience.org.cn/CSTR:20146.11.2021.10.08.V1.

development of satellite remote sensing technology makes it more convenient to monitor SSM at different spatial and temporal scales. Remote sensing methods include optical remote sensing and microwave remote sensing. Optical remote sensing is greatly affected by cloud, rain and other weather conditions, so its application is limited, especially in southern China. Microwave remote sensing has a unique advantage because it has a longer wavelength than visible and infrared wavelengths, and is less affected by bad weather conditions, e.g., clouds and precipitation. Microwave remote sensing is commonly used to monitor SSM, e.g., the Advanced Scatterometer (ASCAT)[8,9], Soil Moisture Ocean Salinity (SMOS)[8,10] and Soil Moisture Active and Passive (SMAP)[8,11,12]. However, the low spatial resolution (about 40 km[13]) cannot meet the requirements of agricultural fine management and efficient use of water resources.

In recent decades, synthetic aperture radar (SAR) have produced significant advantages in estimating soil surface features, especially surface roughness[14] and soil moisture[15]. The SAR images with L, C and X-bands are widely used for SSM estimation[16–19]. Studies by relevant scholars[18,20] show that the C-band sensor carried by Sentinel-1 (S1) shows the inversion ability of soil characteristics on a vegetation covered surface. Sentinel-1 images can be used for both SSM inversion and downscaling of SMOS or SMAP SM. A higher accuracy of SSM can be obtained by using active and passive microwave remote sensing data fusion. Based on the sensitivity of radar backscattering coefficient to SSM, the fitting relationship between the radar backscattering coefficient and soil moisture data from the China Meteorological Administration (CMA) Land Data Assimilation System (CLDAS) was determined to obtain SSM with high spatial resolution. Concurrently, the support vector machine method[21] based on machine learning was used to identify and extract farmland within the study area to obtain a high spatial resolution farmland SSM dataset, which provides support for the fine agricultural management and efficient use of water resources.

2 Survey of the Study Area

The Panzhuang Irrigation District (36°24′N–37°51′N, 116°57′E–115°51′E) is a large-scale irrigation area linked to the Yellow River in China, located west of Dezhou city within Shandong. It is bordered by the Lijia'an Irrigation District to the east, the Yellow River to the south, Dezhou city to the west, Hebei to the northwest, and the Wei canal and Zhangweixin river to the north[22]. The area was built and put to use in 1972. It includes Decheng, Lingcheng, Ningjin, Wucheng, Pingyuan, Xiatjin, Yucheng, and Qihe, with a total area of 5,851 km^2. The maximum annual precipitation is 1,018 mm, the minimum annual precipitation is only 286 mm, and the average annual precipitation is 562 mm. The precipitation from July to September accounts for 65% of the annual precipitation, and the interannual distribution of precipitation in the area is uneven. The average annual evaporation is 1,240 mm. Panzhuang Irrigation District is an important grain and cotton production base in the northwest of Shandong, and provides a large amount of high- quality water resources for Dezhou city, making an essential contribution to the

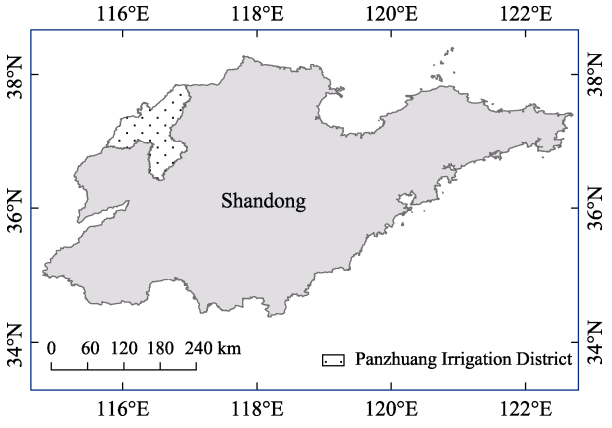

Figure 1 Location map of the Panzhuang Irrigation District within Shandong

economic development and agricultural production in this area[23].

3 Metadata of the Dataset

The metadata for the dataset[24], which includes the full name of the dataset, its short name, the authors, the years, the temporal resolution, data format, data size, data files, data publisher, and data sharing policy are summarized in Table 1.

Table 1 Metadata summary of the 20-m/12-d soil moisture dataset covers Panzhuang Irrigation District of China (2020)

Items	Description
Dataset full name	20-m/12-d soil moisture dataset covers Panzhuang Irrigation District of China (2020)
Dataset short name	SM_Panzhuang_2020
Authors	Wang, J. J., Operation and Maintenance Center of Panzhuang Irrigation District, Dezhou, 1558412182@qq.com Shi, H. J., Water Conservancy Bureau of Dezhou, 1159045384@qq.com Wei, Z., China Institute of Water Resources and Hydropower Research, weizheng@iwhr.com Lin, R. C., China Institute of Water Resources and Hydropower Research, 190453501@qq.com Wang, J., Aerospace Information Research Institute, Chinese Academy of Sciences, wangjin@aircas.ac.cn Zhang, D., China Institute of Water Resources and Hydropower Research, 1945685727@qq.com
Geographical region	Panzhaung Irrigation District
Year	2020
Temporal resolution	12 d
Data format	.tif, .shp
Data size	1.09 GB
Data files	Boundary vector data of Panzhuang Irrigation District; surface soil moisture for 31 12-d periods during 2020, having a temporal resolution of 12 d and a spatial resolution of 20 m
Foundation	Ministry of Science and Technology of P. R. China (2017YFC0403202)
Data computing environment	ArcGIS10.4, ENVI5.6, SARscape5.4
Data publisher	Global change scientific research data publishing system, http://www.geodoi.ac.cn
Address	No. 11A, Datun Road, Chaoyang District, Beijing 100101, China
Data sharing policy	***Data*** from the Global Change Research Data Publishing & Repository includes metadata, datasets (in the *Digital Journal of Global Change Data Repository*), and publications (in the *Journal of Global Change Data & Discovery*). ***Data*** sharing policy includes: (1) ***Data*** are openly available and can be free downloaded via the internet; (2) end users are encouraged to use ***Data*** subject to citation; (3) users, who are by definition also value-added service providers, are welcome to redistribute ***Data*** subject to written permission from the GcdataPR Editorial Office and the issuance of a ***Data*** redistribution license; and (4) if ***Data*** are used to compile new datasets, the 'ten percent principal' should be followed such that ***Data*** records utilized should not surpass 10% of the new dataset contents, and sources should be clearly noted in suitable places in the new dataset[25]
Communication and searchable system	DOI, CSTR, Crossref, DCI, CSCD, CNKI, SciEngine, WDS/ISC, GEOSS

4 Methods

4.1 Data Sources

The data used were Sentinel-1 (S1)[1] SAR images, with a spatial resolution of 20 m. These images were captured using a C-band SAR sensor and an interferometric wide swath mode (IW) with vertical-vertical (VV) polarization and vertical-horizontal (VH) polarization. There are some other auxiliary data, e.g., Landsat8 Operational Land Imager (OLI)[2] images,

[1] https://scihub.copernicus.eu.

boundary vector data of Panzhuang Irrigation District, digital elevation model (DEM)[3] data with a spatial resolution of 90 m and CLDAS SSM[4]. The specific parameters of the S1 images used are shown in Table 2.

Table 2 Parameters for Sentinel-1 (S1) synthetic aperture radar images (IW=interferometric wide swath mode; SLC=single look complex, VV=vertical-vertical polarization; VH=vertical-horizontal polarization)

Images	Date			Imagingmode	Product type	Spatial resolution (m)	Band	Polarization
S1	20200105	20200117	20200129	IW	SLC	20	C	VV/VH
	20200210	20200222	20200305					
	20200317	20200329	20200410					
	20200422	20200504	20200516					
	20200528	20200609	20200621					
	20200703	20200715	20200727					
	20200808	20200820	20200901					
	20200913	20200925	20201007					
	20201019	20201031	20201112					
	20201124	20201206	20201218					
	20201230							

4.2 Data Processing

A flowchart of the farmland SSM mapping process is presented in Figure 2. The S1 images were used as the data source, focusing on the Panzhuang Irrigation District. According to the sensitivity of the backscattering coefficient to SSM, a linear regression model was established. By fitting the coefficient of the backscattering coefficient with SSM derived from CLDAS, SSM values with high spatial resolution were obtained. Concurrently, the support vector machine (SVM) algorithm was used to identify and extract farmland areas, and obtain the SSM values within farmland. These data are highly relevant to water storage management, drought warning, and irrigation planning. SVM classification is a machine learning method based on statistical learning theory. Its decision boundary is the maximum edge hyperplane to solve the learning sample, which solves classification problems involving complex data and is applicable to statistical learning of high-dimensional feature space and small samples[26].

5 Data Results

5.1 Data products

Details regarding the files containing the boundary vector data for the Panzhuang Irrigation District SSM data for 2020 are listed in Table 2. The SSM dataset for the Panzhuang Irrigation District (2020) includes 31 files in .tif format, covering the period from 5 January, 2020 to 30 December, 2020. The dataset has a temporal resolution of 12 d and a spatial resolution of 20 m. The SSM unit in the dataset is cm^3/cm^3, and its value range is (0,1). The files are named using the format: SSM_yyyymmdd.tif, e.g., SSM_20201230.tif indicates SSM data for 30 December, 2020.

5.2 Data Results

Figure 3 shows the comparison of SSM estimation accuracy between winter wheat and summer maize values, determined using different polarization modes during the growing season. In the winter wheat growing season, an important period of Yellow River irrigation

[2] https://www.usgs.gov.

[3] http://www.gscloud.cn.

[4] http://data.cma.cn.

in the Panzhuang Irrigation District, the SSM values are greatly affected by irrigation. In contrast, during the summer maize growing season, they are mainly affected by precipitation. Four days of vigorous crop growth in irrigated areas were selected for comparison (winter wheat: 10 April, 2020 and 6 May, 2020; summer maize: 27 July, 2020 and 20 August, 2020). During the growing seasons of winter wheat and summer maize, the backscattering coefficients of VV polarization were 9–11 db higher than those derived from VH polarization. The ranges of backscattering coefficients of VV and VH polarization modes were (−16, −8) and (−24, −12), respectively.

Table 3 Brief table of the 20-m/12-d SSM dataset for the Panzhuang Irrigation District (2020)

Data	Data format	Data content	Data amount
The boundary of the Panzhuang Irrigation District	.shp	Vector data	32.60 KB
31 SSM data in the Panzhuang Irrigation District in 2020	.tif	SSM data	1.09 GB

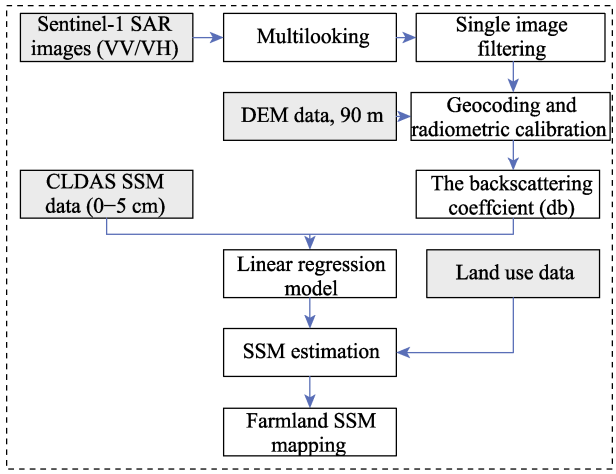

Figure 2 Flowchart for SSM mapping of farmland areas

Differences in SM caused by rainfall versus irrigation for different periods were reflected in differences in backscattering coefficients. Figure 3 shows that on 20 August, 2020, the estimation accuracy of VH polarization was slightly higher than that of VV polarization. On 10 April, 2020, 6 May, 2020, and 27 July, 2020, the estimation accuracy of VV polarization was higher than that of VH polarization, yielding determination coefficients (R^2) of 0.118, 0.033, and 0.136, respectively. Therefore, the backscattering coefficient of VV polarization mode and SSM values from CLDAS were selected to establish a regression model for SSM estimation. The estimation results of SSM were different among different crop types, and the estimation results during the summer maize growing season were better than those during the winter wheat growing season (summer maize: R^2 = 0.505, 0.492; winter wheat: R^2 = 0.444, 0.345).

Figure 4 shows the spatial distribution of SSM obtained for different polarization modes. Four days (27 July, 2020, 8 August, 20 August, and 1 September, 2020) were selected for analysis, representing dates when crops were growing vigorously in the area, within a spatial range of 5 km × 5 km. According to the figure, the removal effect of roads, buildings and other features in the area is obvious. The correlation coefficient (R) for SSM values obtained from inversion of the two polarization modes was between 0.383 and 0.525.

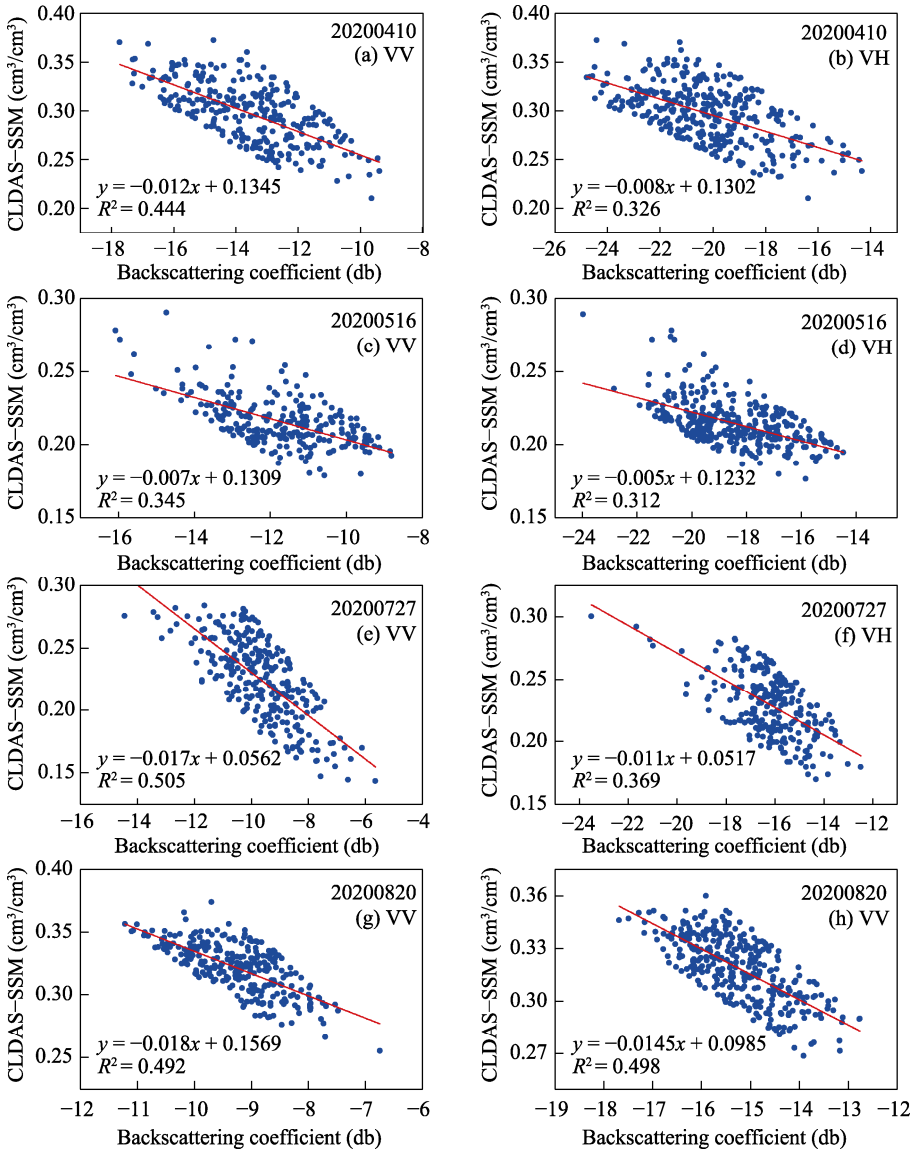

Figure 3 SSM retrieval under different polarization modes during the winter wheat (a–d) and summer maize (e–g) growing seasons

As shown in Figure 5, the SSM estimation method was applied to the Panzhuang Irrigation District. Figure 5a shows farmland SM values in the Panzhuang Irrigation District on 10 April, 2020. The range of SSM values was 0–0.49 cm^3/cm^3, but typically between 0.16–0.36 cm^3/cm^3; Figure 5b shows the farmland SSM values in the Panzhuang Irrigation District on 27 July, 2020. The range of SSM values was 0–0.37 cm^3/cm^3, but typically between 0.14–0.28 cm^3/cm^3. These results are consistent with the SSM values from CLDAS, and provide a reference for irrigation management, drought prediction and crop yield estimation.

6 Discussion and Conclusion

S1 images for SSM retrieval show that VV polarization performs better than VH polarization,

yielding determination coefficients (R^2) between 0.369 and 0.508. The removal effect of roads, buildings and other features in the areas is obvious. The correlation coefficient (R) of SSM obtained from the two polarization methods is between 0.383 and 0.525.

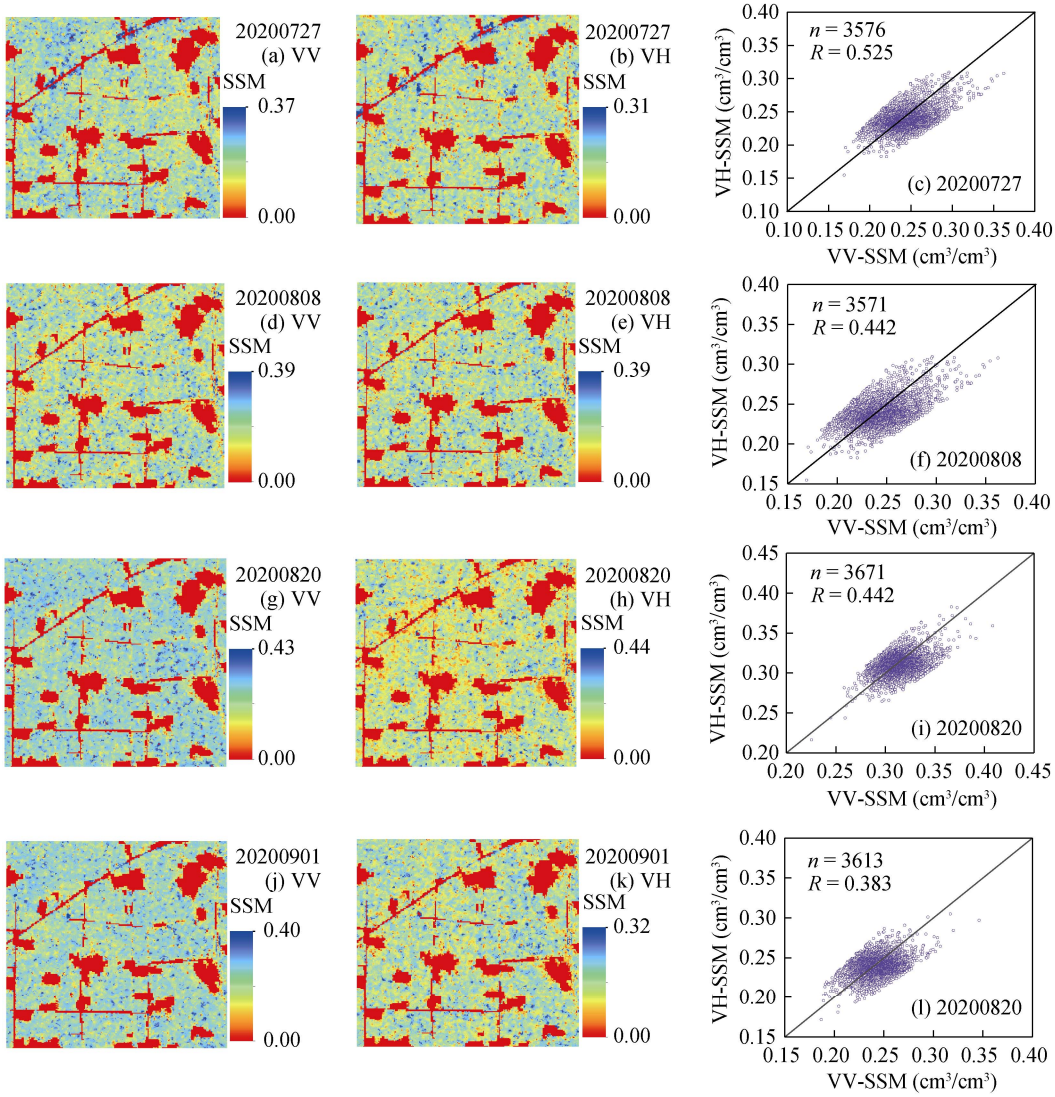

Figure 4 Spatial distribution of SSM derived from different polarization modes

A regression model was established between SSM values from CLDAS and the backscattering coefficient from S1 images. However, the spatial representation of SSM grid pixels with a resolution of 0.0625° × 0.0625° varies greatly, especially in areas with complex underlying surface properties. S1 images have high spatial resolution, and some errors may occur when the backscattering coefficient is resampled to the same resolution as the SSM raster data. In addition, although high spatial resolution SSM data were obtained, the temporal resolution was low and did not meet the requirement for time continuity. In the future, station-based SSM observations could be carried out. Inputting these data into the inversion model would effectively reduce the impact of differences in spatial representativeness. S1 images can be used not only for SSM retrieval[27], but also for SMOS or SMAP SM downsca-

ling[16]. In the future, the data fusion method combining active and passive microwave remote sensing data will be used to obtain SSM data with higher spatial and temporal resolutions.

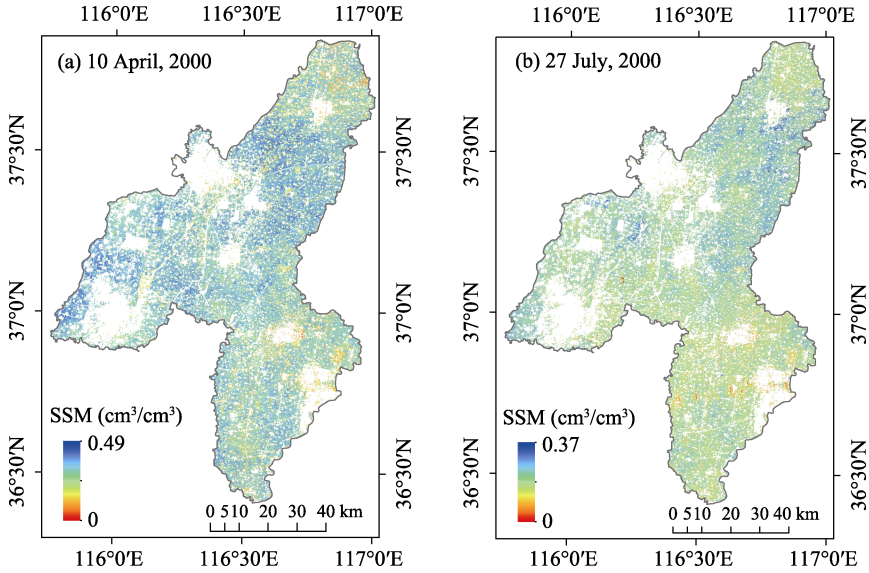

Figure 5 SSM mapping in the Panzhuang Irrigation District for 10 April (a) and 27 July (b), 2020

Author Contributions

Wang, J. J. made the overall design for the development of the dataset; Zhang, D. and Shi, H. J. downloaded and processed the remote sensing data for the Panzhuang Irrigation District; Wei, Z. designed the model algorithm; Lin, R. C. and Wang, J. wrote the paper.

Conflicts of Interest

The authors declare no conflicts of interest.

References

[1] Alizadeh, M. R., Nikoo, M. R. A fusion-based methodology for meteorological drought estimation using remote sensing data [J]. *Remote Sensing of Environment an Interdisciplinary Journal*, 2018, 211: 229–247.

[2] Dorigo, W., Wagner, W., Albergel, C., *et al*. ESA CCI Soil Moisture for improved Earth system understanding: State-of-the art and future directions [J]. *Remote Sensing of Environment*, 2017, 203: 185–215.

[3] Mccoll, K. A., He, Q., Lu, H., *et al.* Short-term and long-term surface soil moisture memory time scales are spatially anticorrelated at global scales [J]. *Journal of Hydrometeorology*, 2019, 20(6): 1165–1182.

[4] Kim, H., Lakshmi, V. Global dynamics of stored precipitation water in the topsoil layer from satellite and reanalysis data [J]. *Water Resources Research*, 2019, 55(4): 3328–3346.

[5] Xu, A. Z., Hu, J. M., Xiong, Y., *et al*. Comparison of soil moisture measurement using TDR method, dry burning method and oven drying method [J]. *Journal of Water Resources and Water Engineering*, 2018, 29(2): 253–256.

[6] Wang, G. S., Shi, H. B., Li, X. Y., *et al*. Simulation and evaluation of soil water and salt transport in desert oases of Hetao Irrigation District using HYDRUS-1D model [J]. *Transactions of the Chinese Society of Agricultural Engineering*, 2021, 37(8): 87–98.

[7] Bai, L. L., Long, D., Yan, L. Estimation of surface soil moisture with downscaled land surface temperatures using a data fusion approach for heterogeneous agricultural land [J]. *Water Resources Research*, 2019, 55(2): 1105–1128.

[8] Zheng, C. L., Hu, G. C., Chen, Q. T., *et al*. Impact of remote sensing soil moisture on the evapotranspiration estimation [J]. *National Remote Sensing Bulletin*, 2021, 25(4): 990–999.

[9] Xie, Q. X., Jia, L., Chen, Q. T., *et al*. Evaluation of microwave remote sensing soil moisture products farming-pastoral area of Shandian river basin [J]. *National Remote Sensing Bulletin*, 2021, 25(4): 974–989.

[10] Merlin, O., Escorihuela, M. J., Mayoral, M. A., *et al*. Self-calibrated evaporation-based disaggregation of SMOS soil moisture: an evaluation study at 3 km and 100 m resolution in Catalunya, Spain [J]. *Remote Sensing of Environment*, 2013, 130: 25–38.

[11] Chan, S. K., Bindlish, R., O'Neill, P., *et al*. Development and assessment of the SMAP enhanced passive soil moisture product [J]. *Remote Sensing of Environment*, 2018, 204: 2539–2542.

[12] Das, N. N., Entekhabi, D., Dunbar, R. S., *et al*. The SMAP mission combined active-passive soil moisture product at 9 km and 3 km spatial resolutions [J]. *Remote Sensing of Environment*, 2018, 211: 204–217.

[13] Zribi, M., Andre, C., Decharme, B. A method for soil moisture estimation in Western Africa based on ERS scatterometer [J]. *IEEE Transactions on Geoscience and Remote Sensing*, 2008, 46(2): 438–448.

[14] Zribi, M., Gorrab, A., Baghdadi, N. A newsoil roughness parameter for themodelling of radar backscattering over bare soil [J]. *Remote Sensing of Environment*, 2014, 152: 62–73.

[15] Gorrab, A., Zribi, M., Baghdadi, N., *et al*. Potential of X-Band TerraSAR-X and COSMO-SkyMed SAR data for the assessment of physical soil parameters [J]. *Remote Sensing*, 2015, 7(1): 747–766.

[16] Gao, Q., Zribi, M., Escorihuela, M. J., *et al*. Synergetic use of Sentinel-1 and Sentinel-2 data for soil moisture mapping at 100 m resolution [J]. *Sensors*, 2017, 17(9): 1966.

[17] Li, J., Wang, S. Using SAR-Derived vegetation descriptors in a Water Cloud Model to improve soil moisture retrieval [J]. *Remote Sensing*, 2018, 10(9): 1370.

[18] Bousbih, S., Zribi, M., El Hajj, M., *et al*. Soil moisture and irrigation mapping in a semi-arid region, based on the synergetic use of Sentinel-1 and Sentinel-2 data [J]. *Remote Sensing*, 2018, 10(12): 1953.

[19] Amazirh, A., Merlin, O., Er-Raki, S., *et al*. Retrieving surface soil moisture at high spatio-temporal resolution from a synergy between Sentinel-1 radar and Landsat thermal data: a study case over bare soil [J]. *Remote Sensing of Environment*, 2018, 211: 321–337.

[20] Bao, Y., Lin, L., Wu, S., *et al*. Surface soil moisture retrievals over partially vegetated areas from the synergy of Sentinel-1 and Landsat 8 data using a modified water-cloud model [J]. *International Journal of Applied Earth Observation and Geoinformation*, 2018, 72: 76–85.

[21] Gao, Q., Zribi, M., Escorihuela, M., *et al*. Irrigation mapping using Sentinel-1 time series at field scale [J]. *Remote Sensing*, 2018, 10(9): 1495.

[22] Li, J. M., Wang, J. J., Yan, Q. H. Analysis of water and soil resources balance in Panzhuang Irrigated Disrrict, Shandong province [J]. *Water Resources Development Research*, 2020, 20(9): 47–50, 58.

[23] Feng, Y. Q., Li, Q. Y., Wang, H. J., *et al*. Analysis on the network scheme of ultrasonic water level system in Panzhuang Irrigation District, Shandong province [J]. *Ground Water*, 2007(4): 117–118.

[24] Wang, J. J., Shi, H. J., Wei, Z., *et al*. 20-m/12-d soil moisture dataset covers Panzhuang Irrigation District of China (2020) [J/DB/OL]. *Digital Journal of Global Change Data Repository*, 2021. https://doi.org/10.3974/geodb.2021.10.08.V1. https://cstr.escience.org.cn/CSTR:20146.11.2021.10.08.V1.

[25] GCdataPR Editorial Office. GCdataPR data sharing policy [OL]. https://doi.org/10.3974/dp.policy.2014.05 (Updated 2017).

[26] Zhang, D. Y., Dai, Z., Xu, X. G., *et al*. Crop classification of modern agricultural park based on time series Sentinel-2 images [J]. *Infrared and Laser Engineering*, 2021, 50(05): 262–272.

[27] Yu, F., Zhao, Y. A new semi-empirical model for soil moisture content retrieval by ASAR and TM data in vegetation-covered areas [J]. *Science China Earth Sciences*, 2011, 54(12): 1955–1964.